Published in final edited form as:
Mol Microbiol. 2010 January ; 75(2): 394–412. doi:10.1111/j.1365-2958.2009.06987.x.

Asymmetric cross regulation between the nitrate-responsive NarX-NarL and NarQ-NarP two-component regulatory systems from *Escherichia coli* K-12

Chris E. Noriega[1], **Hsia-Yin Lin**[2], **Li-Ling Chen**[1], **Stanly B. Williams**[3], and **Valley Stewart**[1,2,*]

[1] Department of Microbiology, University of California, Davis, CA 95616-8665, USA

[2] Food Science Graduate Group, University of California, Davis, CA 95616-8665, USA

[3] Department of Biology, University of Utah, Salt Lake City, UT 84112-0840, USA

Summary

The NarX-NarL and NarQ-NarP sensor-response regulator pairs control *Escherichia coli* gene expression in response to nitrate and nitrite. Previous analysis suggests that the Nar two-component systems form a cross regulation network *in vivo*. Here we report on the kinetics of phosphoryl-transfer between different sensor-regulator combinations *in vitro*. NarX exhibited a noticeable kinetic preference for NarL over NarP, whereas NarQ exhibited a relatively slight kinetic preference for NarL. These findings were substantiated in reactions containing one sensor and both response regulators, or with two sensors and a single response regulator. We isolated 21 NarX mutants with missense substitutions in the cytoplasmic central and transmitter modules. These confer phenotypes that reflect defects in phospho-NarL dephosphorylation. Five of these mutants, all with substitutions in the transmitter DHp domain, also exhibited NarP-blind phenotypes. Phosphoryl-transfer assays *in vitro* confirmed that these NarX mutants have defects in catalyzing NarP phosphorylation. By contrast, the corresponding NarQ mutants conferred phenotypes indicating comparable interactions with both NarP and NarL. Our overall results reveal asymmetry in the Nar cross-regulation network, such that NarQ interacts similarly with both response regulators, whereas NarX interacts preferentially with NarL.

Introduction

Two-component signal transduction involves histidyl-aspartyl phosphoryl-transfer reactions between the transmitter module of a sensor and the receiver domain of a response regulator (Ninfa and Magasanik, 1986); reviewed by (Parkinson and Kofoid, 1992). Specific stimuli control sensor autophosphorylation (transmitter autokinase activity), and the resulting phospho-sensor serves as substrate for response regulator phosphorylation (transmitter phosphotransferase activity) (reviewed by (Stock et al., 1995). Sensor-dependent response regulator phosphorylation occurs at substantially faster rates than does sensor autophosphorylation, so phospho-response regulator formation is governed by phosphoryl flux through the transmitter (reviewed by (Stock et al., 2000). Moreover, for many two-component systems, unphosphorylated sensor stimulates phospho-response regulator dephosphorylation (transmitter phosphatase activity) (reviewed by (Stock et al., 1995). Thus, phsopho-response regulator levels are determined through the relative rates for the transmitter autokinase and transmitter phosphatase reactions (Fig. 1) (reviewed by (Ninfa et al., 1995; Pratt and Silhavy, 1995).

*Corresponding author: Department of Microbiology, University of California, One Shields Avenue, Davis CA 95616-8665, vjstewart@ucdavis.edu, Office: (530) 754-7994, Fax: (530) 752-9014.

Many bacterial species contain dozens of distinct two-component regulatory systems; *Escherichia coli* K-12 has about 30 (Kiil et al., 2005). Some non-cognate transmitter-receiver pairs exhibit relatively weak phosphoryl-transfer reactions *in vitro* (Ninfa et al., 1988; Fisher et al., 1996; Skerker et al., 2005). This **cross talk** (Ninfa et al., 1988) in most cases likely represents "unwanted transfer of signals from one circuit to another" (Wanner, 1992). Remarkably, in wild-type cells, cross talk appears to have negligible impact on signal transduction, for at least two reasons (reviewed by (Hoch and Varughese, 2001; Laub and Goulian, 2007). First, cognate sensor-regulator phosphoryl-transfer reactions exhibit strong kinetic preference over non-cognate interactions (Fisher et al., 1996; Skerker et al., 2008; Groban et al., 2009). This preference is dictated by specificity determinants within both the transmitter and receiver domains (Jiang et al., 1999; Skerker et al., 2008). Second, transmitter phosphatase activity functions to counteract receiver phosphorylation that results from cross talk (Alves and Savageau, 2003; Siryaporn and Goulian, 2008; Groban et al., 2009).

Nevertheless, in some cases non-cognate interactions may influence signaling *in vivo* to form a physiologically-relevant regulatory network. Such **cross regulation** may function to coordinate metabolism or growth (Wanner, 1992). By definition, cross regulation results from response to environmental cues, whereas cross talk does not (Silva et al., 1998); reviewed by (Wanner et al., 1996).

One example of cross regulation is provided by the NarX-NarL and NarQ-NarP two-component regulatory systems (reviewed by (Laub and Goulian, 2007), which control transcriptional response to nitrate and nitrite, the preferred anaerobic electron acceptors (reviewed by (Stewart and Rabin, 1995; Stewart, 2003). Phosphorylation of the NarL and NarP response regulators is governed by the NarX and NarQ sensors in response to signal ligands, nitrate and nitrite (Fig. 1). Analysis of null mutants reveals that either the NarX or the NarQ sensor is sufficient for NarL-dependent activation of *narGHJI* operon transcription (Egan and Stewart, 1990; Chiang et al., 1992; Rabin and Stewart, 1992). These and similar observations with other NarL- and NarP-regulated operons provide *in vivo* evidence that the Nar regulators form a signal-responsive cross regulation network (reviewed by (Stewart and Rabin, 1995). This previous model, which assumes essentially equivalent transmitter phosphotransferase interactions between different sensor-regulator combinations, depicts a symmetrical core interaction network, with differences mainly in input (nitrate vs. nitrite) and output (distinct sets of target operons).

Here, we present results from biochemical and genetic experiments to examine core sensor-regulator interactions directly. Results reveal that that this core interaction network is asymmetric (Fig. 1): although the NarQ sensor exhibited similar transmitter phosphotransferase activities for both the NarP and NarL response regulators, the NarX sensor by contrast exhibited a marked preference for phosphotransfer to NarL. These preferences were particularly evident in reactions containing one sensor and both regulators. Among a collection of NarX missense mutants identified as having defective transmitter phosphatase activity for NarL, five displayed an additional NarP-blind phenotype. *In vitro*, the mutant proteins were defective in transmitter phosphotransferase activity for NarP but retained near-normal activity for NarL. These mutational changes lie in a region of the dimerization and histidyl-phosphotransfer (DHp) domain that recently, in other sensors, has been implicated as important for determining specificity for transmitter-receiver interactions. By contrast, the corresponding substitutions in the NarQ sensor yielded mutants with essentially equivalent NarL- and NarP-dependent regulatory phenotypes. Together, these findings show that the NarX sensor is more specialized for interaction with the NarL regulator, whereas the NarQ sensor is more generalized for interaction with either the NarP or the NarL regulators (Fig. 1).

Results

Phosphoryl-transfer time-course reactions

Although many two-component sensors are intrinsic membrane proteins, their transmitter modules reside in the cytoplasm. Thus, *in vitro* studies of sensor-response regulator interactions often use sensor proteins lacking the amino-terminal transmembrane portion. One of the best-characterized sensors, EnvZ, has been studied *in vitro* predominantly as a soluble form lacking the intact periplasmic and transmembrane domains (Igo et al., 1989; Mattison and Kenney, 2002; Yoshida et al., 2002). Moreover, recent detailed studies examining cognate and non-cognate interactions between the EnvZ-OmpR, CpxA-CpxR and RstB-RstA systems likewise have used transmembrane region-deleted sensors, with either carboxyl-terminal His_6 (Groban et al., 2009) or amino-terminal His_6-MBP tags (Skerker et al., 2008). Similarly, detailed analysis of VanS sensor interaction with the VanR and PhoB regulators used protein in which the amino-terminal transmembrane region was replaced with MBP (Fisher et al., 1996).

Accordingly, for this study we used sensor proteins for which the periplasmic and transmembrane domains have been replaced with MBP (Noriega et al., 2008). Even though activities are not modulated in response to signal ligand, these proteins displayed robust autokinase, phosphotransfer and phosphatase activities to enable analysis of relative kinetic preferences and effects of mutational alterations.

Phosphoryl-transfer involving MBP-Nar sensors and His_6-Nar response regulators was examined by using Laemmli gel electrophoresis to separate the proteins (examples shown in Fig. 2E). Time-course assays initiated with phosphorylated sensor monitor both subsequent transmitter reactions, phosphotransferase and phosphatase.

Assays reported here differed in two ways from previous analyses of Nar phosphoryl-transfer reactions (Walker and DeMoss, 1993; Schröder et al., 1994; Yamamoto et al., 2005). First, previous assays were conducted at pH 8. However, the NarQ autophosphorylation rate is faster at pH 7, where it compares with the NarX rate at either pH value (Noriega et al., 2008); and **data not shown**). Therefore, all experiments reported here were conducted at pH 7. Second, previous assays contained limiting ATP and/or inhibitory ADP concentrations. Nar sensor autophosphorylation is rapidly reversible, reflecting high affinity for ADP (Noriega et al., 2008); and **data not shown**). Evidence suggests that the ADP contamination in ATP stocks is sufficient to inhibit phospho-sensor accumulation, and indeed, increasing ATP concentration results in decreasing levels of accumulated phospho-Nar sensor (Williams and Stewart, 1997b; Lee et al., 1999); and **data not shown**). Accordingly, experiments reported here were conducted either with phospho-MBP-Nar sensors that had been isolated free from nucleotides (single-round reactions), or in the presence of ATP-regeneration (multiple-round reactions).

We determined the optimal sensor to regulator ratio by performing reactions with 0.5 μM (dimers) of MBP-Nar sensors and different concentrations of His_6-Nar response regulators (0.5, 1, 5 and 10 μM monomers). These assays included ATP-regeneration. For all four combinations, the levels of phosphorylated regulator increased between 0.5 and 5 μM, but did not increase further at 10 μM (**data not shown**). Therefore, all time-course experiments described below used sensors and regulators at 0.5 μM (dimers) and 10 μM (monomers), respectively. This ratio follows the notion that the in vivo level of a response regulator is higher than that of its cognate sensor (Cai and Inouye, 2002).

Single-round phosphoryl-transfer time-course reactions

In single-round reactions free from ATP, the sensor remains dephosphorylated after phosphotransfer to the regulator. Time-course patterns for three combinations were similar: MBP-NarX and His_6-NarL (Fig. 2A), MBP-NarQ and His_6-NarL (Fig. 2C), and MBP-NarQ and His_6-NarP (Fig. 2D). In each case, radiolabeled sensor was depleted within 5 min after the addition of response regulator. Phospho-regulator accumulated transiently to low levels, and was subsequently depleted. This pattern suggests relatively strong transmitter phosphotransferase and phosphatase activities for these sensor-regulator pairs. By contrast, radiolabeled MBP-NarX was depleted more slowly upon addition of His_6-NarP, and phospho-His_6-NarP persisted for a longer duration (Fig. 2B; and **data not shown**). This pattern suggests relatively weak transmitter phosphotransferase and phosphatase activities for this pair.

Multiple-round phosphoryl-transfer time-course reactions

Due to the rapid loss of radiolabel from phospho-response regulators in the single-round reactions described above, we decided also to perform phosphoryl-transfer reactions in the presence of ATP and ATP-regeneration. In these reactions, phosphorylated sensor is regenerated after phosphotransfer, and so reactions can approach an equilibrium governed by the relative rates of both sensor and response regulator phosphorylation and dephosphorylation.

The interaction between MBP-NarX and His_6-NarL in the multiple-round reactions (Fig. 3A) was similar to that in the single-round reactions (Fig. 2A): radiolabeled MBP-NarX was rapidly depleted, indicating that the transmitter phosphotransferase rate is significantly faster than the transmitter autokinase rate. Phospho-His_6-NarL did not accumulate, likely due to slower His_6-NarL phosphorylation (limited by relatively slow MBP-NarX autophosphorylation) compared to phospho-His_6-NarL dephosphorylation.

By contrast, interaction between MBP-NarX and His_6-NarP in the multiple-round reactions (Fig. 3B) was different from that in the single-round reactions (Fig. 2B), because phospho-His_6-NarP continued to accumulate throughout the multiple-round time-course. This pattern indicates slower phospho-His_6-NarP dephosphorylation compared to His_6-NarP phosphorylation.

Likewise, a different pattern emerged for multiple-round reactions with MBP-NarQ and either His_6-NarL (Fig. 3D) or His_6-NarP (Fig. 3E). In both cases, phospho-His_6-NarL and phospho-His_6-NarP persisted, but did not continue to accumulate throughout the time-course. This contrasts with the single-round reactions, in which the phospho-response regulators were depleted rapidly (Figs. 2C & D). Thus, these multiple-round reactions achieved a balance between response regulator phosphorylation and dephosphorylation. The persistence of phosphorylated regulator in the multiple-round reactions with MBP-NarQ may result in part from the more rapid rate of MBP-NarQ autophosphorylation compared to that for MBP-NarX (Noriega et al., 2008).

Multiple-round phosphoryl-transfer time-course reactions with two response regulators

Interactions between one sensor and both response regulators were examined by adding a 1:1 mixture (final concentration of 5 μM monomers of each) of His_6-NarL (25 kDa) plus MBP-NarP (66 kDa) to the phosphorylated sensor (82–85 kDa). The three proteins were readily resolved by Laemmli gel electrophoresis to enable individual quantification. Control experiments established that phosphorylated MBP-NarP, His_6-NarP, and NarP (generated by factor Xa cleavage of MBP-NarP) accumulated at indistinguishable rates in reactions with MBP-NarX (**data not shown**).

In multiple-round reactions with MBP-NarX (Fig. 3C), phosphoryl transfer to His_6-NarL was similar to that observed in single-regulator reactions (see Fig. 3A), whereas radiolabeled MBP-NarP was not detected. This pattern indicates a substantial phosphotransferase kinetic preference of MBP-NarX for NarL over NarP.

In multiple-round reactions with MBP-NarQ, phospho-His_6-NarL accumulated to much higher levels than phospho-MBP-NarP (Fig. 3F). We hypothesized that contined accrual of phospho-His_6-NarL over the time-course was due in large measure to preferential reaction with phospho-MBP-NarP in the transmitter phosphatase reaction. Indeed, in single-round reactions (**data not shown**), phospho-His_6-NarL accumulated transiently in a pattern similar to that shown in Fig. 2C, whereas lower levels of phospho-MBP-NarP had dissipated by the 2 min time-point. Together, these results suggest that MBP-NarQ has a small kinetic preference for His_6-NarL in the transmitter phosphotransferase reaction, and a larger preference for His_6-NarP in the transmitter phosphatase reaction. This latter conclusion is supported further by separate experiments to measure the transmitter phosphatase rates directly (C. E. Noriega, H.-Y. Lin, L.-L. Chen & V. Stewart, manuscript in preparation).

Multiple-round phosphoryl-transfer time-course reactions with two sensors

Next, we examined the influence of both Nar sensors on one Nar response regulator. To accomplish this, we initiated multiple-round phosphoryl transfer reactions first with one MBP-Nar sensor (phosphorylated) and one His_6-Nar response regulator. Immediately after the 5 min reaction sample was withdrawn, the second MBP-Nar sensor (unphosphorylated) was added to a final concentration also of 0.5 μM dimers. For control reactions, buffer was added instead.

Addition of MBP-NarQ increased the level of phospho-His_6-NarL formed from MBP-NarX(Fig. 4A), whereas addition of MBP-NarX transiently increased then decreased the level of phospho-His_6-NarL formed from MBP-NarQ (Fig. 4C). In both cases, the final level of phospho-His_6-NarL was about the same, about 0.5 pmol of monomers. Thus, the two sensors together result in a level of phospho-His_6-NarL that is intermediate between those with either sensor alone.

Addition of MBP-NarX had little effect on the level of phospho-His_6-NarP formed from MBP-NarQ (Fig. 4D). By contrast, addition of MBP-NarQ resulted in a transient decrease in the level of phospho-His_6-NarP formed from MBP-NarX, followed by a return to the initial level (Fig. 4B). This pattern presumably reflects initial phospho-His_6-NarP dephosphorylation by unphosphorylated MBP-NarQ.

Transmitter phosphotransferase kinetic preferences

Results described above indicate that MBP-NarQ exhibited a slight kinetic preference for phosphotransfer to His_6-NarL over His_6-NarP, whereas MBP-NarX displayed a more pronounced preference for His_6-NarL. We initially sought to quantify this by performing standard Michaelis-Menten analysis. However, as observed with other two-component systems, the phosphotransferase rates were too fast to be measured precisely without rapid quench methods (Fisher et al., 1996; Janiak-Spens et al., 2005; Groban et al., 2009), an approach beyond the scope of our current work. (Our separate measurements of transmitter phosphatase reaction rates will be reported elsewhere; C. E. Noriega. L.-L. Chen & V. Stewart, manuscript in preparation.)

Skerker, Laub and coworkers recently introduced a simple means to compare relative kinetic preferences for phosphotransferase reactions (Skerker et al., 2005; Skerker et al., 2008). In this approach, estimates for the reaction rates are taken to represent the ratio of specificity constants (k_{cat}/K_M) of a given sensor for two different response regulators. Because cognate

phosphotransferase reactions are fast, the measured initial rates explicitly are defined as lower-bound estimates, and thus the resulting ratios provide only order-of-magnitude differences in substrate specificities (Skerker et al., 2008). Nevertheless, values for the kinetic preferences of EnvZ for OmpR over CpxR, and of CpxA for CpxR over OmpR, estimated by Skerker *et al*. (2008) to be about 20,000-fold each, compare well with the rates determined from rapid quench methods, 33,000-fold and 9,300-fold, respectively (Groban et al., 2009).

We adapted this approach as described in Experimental Procedures. Estimated initial rates (V_0) were: MBP-NarX plus His_6-NarL, 0.006 s^{-1}; MBP-NarX plus His_6-NarP, 0.0008 s^{-1}; MBP-NarQ plus His_6-NarL, 0.015 s^{-1}; and MBP-NarQ plus His_6-NarP, 0.005 s^{-1}. These result in estimates for relative kinetic preferences of 1.0 for MBP-NarQ plus His_6-NarL, 0.4 for MBP-NarX plus His_6-NarL, 0.33 for MBP-NarQ plus His_6-NarP, and 0.053 for MBP-NarX plus His_6-NarP. These estimates are congruent with the qualitative conclusions drawn from data presented in Figs. 2–4, that MBP-NarQ had a modest phosphotransferase preference for His_6-NarL over His_6-NarP (estimated here to be about threefold), whereas MBP-NarX had a more pronounced preference for His_6-NarL (estimated here to be about eightfold).

NarX missense substitutions that affect cross regulation

In order to evaluate the above conclusions independently, we analyzed missense substitution mutants that selectively alter NarX transmitter recognition of the NarP receiver domain. These mutants were isolated in a previously-described screen for nitrite-hypersensitive mutants (Williams and Stewart, 1997a, b). In *narX*$^+$ strains, nitrite only weakly induces Φ(*narG-lacZ*) expression (see Table 1). Mutants that confer the nitrite-hypersensitive phenotype likely have diminished transmitter phosphatase activity (Williams and Stewart, 1997a, b). As described below, a subset of these mutants exhibited an additional, unanticipated NarP-blind phenotype, being unable to activate expression of the NarP-dependent *napF* operon.

For this study, we analyzed nitrite-hypersensitive *narX* alleles isolated by mutagenesis of the regions encoding the central and transmitter modules. Error-prone PCR mutagenesis was performed on defined segments of an allele, termed *narX*†, that contains silent restriction endonuclease sites (Williams and Stewart, 1997a). We characterized 21 distinct alleles (Table 1), most of which have alterations in or near distinct sequence motifs within the transmitter DHp domain (H and X box regions) or catalytic and ATP-binding (CA) domain (D or G box regions; sequence motifs are described in references (Wolanin et al., 2002; Hsing et al., 1998). Five alleles have substitutions in two codons. Wild-type and mutant *narX* alleles were present on plasmids that, in the *pcnB1* strain backgrounds used, have low copy numbers (Liu and Parkinson, 1989).

NarX mutant phenotypes for NarL- and NarP-dependent output

We evaluated all mutants for effects on NarL- and NarP-dependent reporter gene expression, and then chose representatives for further analysis as described below. We focused our subsequent effort on the NarP-blind mutants.

Phospho-NarL-dependent gene expression was analyzed by measuring Φ(*narG-lacZ*) expression. Sixteen alleles conferred the nitrite-hypersensitive phenotype (Table 1), defined previously as an increased response to nitrite availability without concomitant increase in basal Φ(*narG-lacZ*) expression or significant defect in nitrate response (Williams and Stewart, 1997a). Among these mutants, nitrite induction was increased from three- to 13-fold over the wild-type level. Three other alleles (I343T, W442C and W442G) conferred

elevated basal Φ(*narG-lacZ*) expression along with nitrite-hypersensitivity. Functionally, two of these mutant alleles (W442C and W442G) and four of the nitrite-hypersensitive alleles (R333L, K410E, M411T and W442R) did not distinguish between nitrate and nitrite availability. Finally, two alleles were unique. One (V580A+F589I) conferred an impaired induction phenotype, because nitrate response was reduced twofold, whereas the other (S508C+D558V) bestowed high-level constitutive Φ(*narG-lacZ*) expression.

Phospho-NarP-dependent gene expression was analyzed by measuring Φ(*napF-lacZ*) expression. The $narX^{\dagger}$ allele confers high-level basal expression, with the consequence that nitrate and nitrite induction is only three- to four-fold (Williams and Stewart, 1997a, b); see Table 1). Phenotypic classes distinct from the NarL interaction classes described above were identified. Five alleles (S405P, M411V, C415R, S508C+D558V and V580A+F589I) conferred an impaired induction phenotype, defined by an inability to raise Φ(*napF-lacZ*) expression levels above the wild-type basal level even under inducing conditions (Table 1). Three alleles (Q350R+T372A, W442C and Y551F) bestowed high-level constitutive Φ(*napF-lacZ*) expression, whereas eight alleles conferred near-normal patterns of Φ(*napF-lacZ*) expression.

The final class, which includes five alleles (K410E, M411T, Q412R+V413M, W442R and F452Y), defines a distinct NarP-blind phenotype. For these mutants, basal-level Φ(*napF-lacZ*) expression was at the low level equivalent to that in the *narX* null strain, and induction by nitrate ranged from negligible to weak (Table 1).

A subset of NarX mutants characterized further *in vivo*

Representative mutant alleles representing the range of phenotypes were chosen for further tests *in vivo*: the phenotypically-unique S508C+D558V and V580A+F589I alleles; the M411T, M411V, C415R, W442R, and F452Y alleles representing a range of nitrite-hypersensitive and NarP interaction phenotypes; the R333L and Y551F alleles, which are the most nitrite-hypersensitive alleles that bestowed either wild-type or constitutive patterns of NarP-mediated gene expression, respectively; and the W442G allele, which conferred increased basal and nitrite-induced NarL-dependent expression while retaining nearly wild type NarP interaction. Tests were performed and analyzed as described previously (Williams and Stewart, 1997a, b).

We expected these mutants to be defective for negative function, which results from phospho-NarL phosphatase activity. We tested this in a strain carrying the *narL505* (V88A) allele, which confers Nar sensor-independent constitutive Φ(*narG-lacZ*) expression (Egan and Stewart, 1991) and the product of which requires phosphorylation for DNA binding (Li et al., 1994). Negative function is revealed upon introduction of the $narX^{+}$ allele, which reduces the uninduced level of Φ(*narG-lacZ*) expression by more than twofold (Rabin and Stewart, 1992; Williams and Stewart, 1997a). Despite the variety of phenotypes concerning positive interactions with the Nar response regulators, all of the tested NarX mutants displayed sharply reduced transmitter phosphatase activity as monitored through the NarL(V88A) phenotype (**data not shown**).

The above tests examined haploid phenotypes in *narX narQ* double null strain backgrounds. We therefore examined the representative *narX* alleles in both $narX^{+}$ *narQ* null and *narX* null $narQ^{+}$ strain backgrounds, to determine dominance relationships and to uncover potential Nar sensor interactions.

Most of the $narX^{+}$/*narX* diploids exhibited two- to sevenfold reduced nitrite-hypersentivitity in comparison to the corresponding mutant homozygotes (**data not shown**). Thus, these alleles lie on a continuum from codominant to recessive, but none were dominant. Overall

complementation behavior correlated with neither the phenotype nor the location of the substitution. Recessive behavior in complementation tests generally indicates loss of function, consistent with our conclusion that these mutants have diminished transmitter phosphatase activity.

Finally, the phenotypes of the *narQ*$^{+}$/*narX* diploids were again consistent with defective transmitter phosphatase activity, as the mutant *narX* alleles failed to reduce NarQ-mediated Φ(*narG-lacZ*) expression in response to nitrite (**data not shown**). Moreover, none of the *narX* mutant alleles interfered with NarQ-NarP control of Φ(*napF-lacZ*) expression. All mutant alleles examined therefore are denoted as functionally recessive to *narQ*$^{+}$. This and previous results (Williams and Stewart, 1997a) imply that any apparent interactions between the two Nar sensors can be attributed to their independent interactions with the Nar response regulators.

Distinct phenotypes conferred by the separate Q412R and V413M substitutions

One of the NarP-blind alleles contains substitutions at adjacent residues (Q412R and V413M). In order to ascertain contributions of the individual alterations to phenotype, we used site-specific mutagenesis to revert each of the substitutions individually. The resulting single mutants were evaluated for positive control of NarL and NarP function *in vivo* (Table 3). Patterns of Φ(*narG-lacZ*) expression show that the V413M mutant phenotype mimicked the strong nitrite-hypersensitive phenotype of the doubly-substituted original, whereas the Q412R mutant displayed only a mild nitrite-hypersensitive phenotype. By contrast, patterns of Φ(*napF-lacZ*) expression reveal that both single substitutions conferred NarP impaired-induction phenotypes that did not fully recapitulate the NarP-blind phenotype of the doubly-substituted original. Accordingly, we used the original Q412R+V413M allele for further study.

NarP-blind mutants: transmitter autokinase activity *in vivo*

One possible explanation for the NarP-blind phenotype is that the mutational alterations cause a severe deficiency in NarX transmitter autokinase activity. In response to ligand availability, such defective NarX proteins would negotiate only slight increases in phospho-NarL and phospho-NarP levels. Slight increases would be insufficient to manifest NarP-mediated Φ(*napF-lacZ*) expression but still reflect near-normal control of NarL-mediated Φ(*narG-lacZ*) expression. (Recall that these mutant alleles have lost their negative function with respect to NarL-mediated transcription.)

To test this *in vivo*, we exploited observations suggesting that *narG* operon expression responds well to relatively low phospho-NarL levels, whereas significant repression of *frdA* operon expression apparently requires relatively high phospho-NarL levels (reviewed by (Stewart and Rabin, 1995). Thus, we reasoned that defective transmitter autokinase would manifest as inefficient Φ(*frdA-lacZ*) repression (Fig. 1).

The *narX*† allele caused threefold repression of Φ(*frdA-lacZ*) expression in response to nitrate but not nitrite (Table 2). As a control, we included the S508C+D558V allele, which conferred a strong NarL-constitutive phenotype (Table 1). In this mutant, Φ(*frdA-lacZ*) expression was at the repressed level under all growth conditions tested, consistent with the constitutively-active transmitter autokinase phenotype exhibited by the S508C+D558V allele.

The two strongest NarP-blind *narX* mutant alleles, M411T and W442R, repressed Φ(*frdA-lacZ*) expression in response to both nitrate and nitrite, consistent with their nitrite-hypersensitive phenotype (Table 2). Therefore, these NarX mutants have near-normal transmitter autokinase activity *in vivo*.

NarP-blind mutants: transmitter autokinase activity *in vitro*

Among the NarP-blind mutants, the M411T, Q412R+V413M and W442R alleles were unable to raise Φ(*napF-lacZ*) expression above that observed in the *narX narQ* double null strain, whereas the K410E and F452Y alleles engendered low levels of induction in response to nitrate and nitrite (Table 1). We denote these as strong and weak NarP-blind phenotypes, respectively. Each of these mutants was recloned to form MBP-NarX hybrid proteins and isolated by affinity enrichment as described in Experimental Procedures.

We monitored autophosphorylation in the presence of ATP-regeneration as described previously (Noriega et al., 2008). Two of the strong NarP-blind mutant proteins, M411T and W442R, were similar to the wild-type, approaching the steady-state level of phosphorylation (about 50% of dimers) by 10 min (Fig. 5A). These results are fully consistent with those from the *in vivo* test for autokinase activity described immediately above. The other strong-phenotype mutant protein (Q412R+M413V) was less active, reaching a substantially lower steady-state (about 20% of dimers) after 20 min. Finally, the two weak-phenotype mutant proteins, F452Y and K410E, required more than 45 min to reach a level of about 40% phosphorylated dimers. Overall, even though some mutant proteins displayed differences from the wild-type autophosphorylation pattern *in vitro*, each was able to accumulate to a phosphorylation level sufficient for further analysis.

We also examined the influence of ADP, by performing reactions without ATP-regeneration. Four mutant proteins displayed the wild-type pattern, with sharply lower steady-state phosphorylation levels. Surprisingly, autophosphorylation by the F452Y mutant protein was much less influenced by ADP (Fig. 2B). We would have anticipated that ADP-sensitivity could be influenced by mutational alterations within the CA domain, affecting relative affinities for ADP vs. ATP (Noriega et al., 2008). However, this result shows that changes near the autokinase active site can (also) influence the rate of phosphotransfer to ADP. We did not pursue this observation for the present study.

NarP-blind mutants: phosphoryl-transfer reaction conditions

In the MBP-NarX phosphoryl-transfer time-course assays conducted near room temperature (19°C), phospho-His_6-NarL accumulated only transiently (Figs. 2 & 3). In order to facilitate comparison between wild-type and mutant sensors, we sought to slow the reaction rates by performing time-course reactions at 4°C. MBP-NarX proteins were autophosphorylated by incubation with [γ-^{32}P] ATP at 19°C for 45 min as described above, and then equilibrated to 4°C. Reactions were initiated by adding His_6-NarL or His_6-NarP.

Although these reactions were performed in the presence of ATP and ATP-regeneration, in separate experiments we observed that wild-type MBP-NarX autophosphorylation was extremely slow at 4°C (**data not shown**). (By contrast, the MBP-NarQ autophosphorylation rate was little affected by temperature.) We therefore infer that phospho-MBP-NarX was not regenerated significantly, and therefore that the time-courses described below effectively were single-round reactions.

NarP-blind mutants: NarL phosphorylation and dephosphorylation

The rates of MBP-NarX-catalyzed His_6-NarL phosphorylation were similarly rapid at both temperatures tested, but dephosphorylation was notably slower at the lower temperature (Figs. 2A & 6A). Thus, phospho-His_6-NarL accumulated to a higher level, and persisted for a longer time, in the reactions performed at 4°C.

The NarP-blind mutant proteins catalyzed rapid, essentially wild-type rates of His_6-NarL phosphorylation (Fig. 6). One possible exception was the W442R mutant, which exhibited

an obviously slower rate of phospho-MBP-NarX depletion (Fig. 6C). Note that differences in phospho-His_6-NarL levels reflect differences in the initial amounts of phospho-MBP-NarX, due to their different autophosphorylation efficiencies (Fig. 5A).

By contrast, four of the mutant proteins exhibited negligible rates of phospho-His_6- NarL dephosphorylation, whereas the K410E mutant catalyzed dephosphorylation at roughly one-half the wild-type rate. Overall, these results are fully consistent with conclusions drawn from the *in vivo* analyses described above (Table 1), that these NarX mutants have active transmitter phosphotransferase but defective transmitter phosphatase activites with NarL as substrate.

NarP-blind mutants: NarP phosphorylation and dephosphorylation

The wild-type MBP-NarX protein catalyzed slower His_6-NarP phosphorylation (approximately 0.35 pmol min^{-1}) at the lower temperature (Fig. 6A) compared to the room-temperature reactions described above (Fig. 2B). Nevertheless, phospho-His_6-NarP accumulated to a similar level as phospho-His_6-NarL (approximately 1 pmol; Fig. 6A). In turn, phospho-His_6-NarP was only slightly depleted over the 20 min time-course, reflecting somewhat slower transmitter phosphatase activity also at the lower temperature (Figs. 2B & 6A; and **data not shown**).

The three strong-phenotype mutant proteins, M411T (Fig. 6B), W442R (Fig. 6C), and Q412R+M413V (Fig. 6D), displayed undetectable phosphotransfer to His_6-NarP. The two weak-phenotype mutants, F452Y (Fig. 6F) and K410E (Fig. 6E), catalyzed His_6-NarP phosphorylation very slowly (approximately 0.02 pmol min^{-1}) and somewhat slowly (approximately 0.1 pmol min^{-1}), respectively.

Overall, these results fully substantiate conclusions drawn from the *in vivo* analyses described above, that these NarX mutants have undetectable (M411T, W442R, and Q412R +V413M) or defective (K410E and F452Y) transmitter phosphotransferase activites with NarP as substrate.

Missense substitutions in the NarQ DHp domain

The striking phenotypes conferred by the NarP-blind alterations in NarX led us to examine analogous substitutions in NarQ. We used site-specific mutagenesis to make changes at residues corresponding to three of the positions that yielded single-substitution NarP-blind alterations in NarX (Fig. 3). Thus, the NarQ R381E, Y413R and F423Y substitutions correspond to the NarX K410E, W442R and F452Y substitutions, respectively. We also used randomized-codon mutagenesis to isolate additional changes at NarQ codons Arg-381 and Ser-382, corresponding to NarX codons Lys-410 and Met-411, respectively. Mutants were identified by screening for altered Φ(*narG-lacZ*) expression as described in Experimental Procedures. The resulting *narQ* mutants were assayed for effects on NarL- and NarP-dependent gene expression as described above for *narX* mutants. (We did not monitor nitrite-dependent expression, because the NarQ sensor mediates similar levels of response to both nitrate and nitrite.)

Overall, phenotypes with respect to NarL- and NarP-dependent expression were similar (Table 4). The Y413R mutant was strongly defective for both NarL- and NarP-dependent expression. Three mutants (I382G, I382S and F423Y) conferred high-level constitutive Φ(*napF-lacZ*) expression and elevated basal Φ(*narG-lacZ*) expression. Among the remaining mutants, three (R381E, R381V, and I382M) exhibited modest constiutive phenotypes (Table 4) whereas nine others (R381G, R381N, R381L, R381W, R381T, R381H, I382F, I382L and I382W) had phenotypes only subtly different from the wild-type

(**data not shown**). Thus, none of the mutants examined displayed notably different phenotypes with respect to NarL- and NarP-dependent output.

Discussion

The NarX-NarL and NarQ-NarP two-component systems are ancient paralogs that likely evolved to control transcription of the *narG* operon and the *napF* plus *nrfA* operons, respectively (Stewart, 2003; Price et al., 2008). The *narQ* and *narP* genes are present mostly in the *Gammaproteobacteria*, including most species in the families *Pasteurellaceae*, *Shewanellaceae*, and *Vibrionaceae*. By contrast, the *narX* and *narL* genes are distributed broadly but sporadically among species in both the *Betaproteobacteria* and *Gammaproteobacteria*, probably through lateral gene transfer of the *narXL–narK–narGHJI* cluster (Stewart, 2003; Price et al., 2008).

Relatively few species, mostly in the family *Enterobacteriaceae*, contain both Nar regulatory systems. *E. coli* and close relatives encode a rich complement of anaerobic respiratory enzymes specialized for distinct niches (Gennis and Stewart, 1996). Thus, it is hypothesized that the NarX-NarL and NarQ-NarP systems interact to fine-tune respiratory enzyme synthesis in response to dynamic equilibria of nitrate and nitrite concentrations (Rabin and Stewart, 1993; Stewart et al., 2002); reviewed by (Stewart and Rabin, 1995). In *E. coli*, the NarX sensor is specialized for preferential response to nitrate, whereas the NarQ sensor is generalized for response to nitrate, nitrite, and other signals (Rabin and Stewart, 1993; Williams and Stewart, 1997b; Lee et al., 1999; Stewart et al., 2003).

Studies with null mutants show that either NarX or NarQ is sufficient for essentially normal nitrate-responsive expression of NarL-dependent operons (Egan and Stewart, 1990; Chiang et al., 1992; Rabin and Stewart, 1992). However, although NarX alone can control NarP-dependent expression, its precise role relative to that of NarQ has been obscure (Rabin and Stewart, 1993; Williams and Stewart, 1997a, b; Stewart and Bledsoe, 2003). This is due in part to the lower output ratio for NarP-dependent gene expression (tenfold or less) compared to that for NarL-dependent *narG* operon expression (about 100-fold; see Table 1), and in part to the complication that expression of NarP-dependent operons is also regulated by NarL. Consequently, models for Nar cross regulation simply have depicted both sensors as catalyzing essentially equivalent rates of phosphotransfer to both response regulators (Rabin & Stewart, 1993); reviewed by (Stewart & Rabin, 1995).

Results presented in this study (1) establish relatives roles for NarX and NarQ in controlling NarL and NarP phosphorylation state, and thereby illuminate the nature and extent of the Nar cross regulation network; and (2) advance understanding of specificity determinants that control cognate and non-cognate transmitter-receiver interactions.

NarX and NarQ act similarly to control NarL phosphorylation

Soluble forms of NarX and NarQ have been shown previously to catalyze efficient NarL phosphorylation and dephosphorylation *in vitro* (Walker and DeMoss, 1993; Schröder et al., 1994; Cavicchioli et al., 1995; Yamamoto et al., 2005). Here, MBP-NarX and MBP-NarQ phosphotransferase and phosphatase activities were indistinguishable in single-round time-course reactions (Figs. 2A & C). Likewise, similar missense substitutions in the NarX and NarQ DHp domains had comparable effects on NarL-dependent gene expression (Tables 1 & 4).

By contrast, in multiple-round reactions where phospho-sensor is regenerated, MBP-NarX appeared to have stronger phospho-His_6-NarL phosphatase activity compared to MBP-NarQ (Figs. 3A & D; Figs. 3A & C). However, interpretation is complicated by the faster rate of

MBP-NarQ autophosphorylation (Noriega et al., 2008). Phospho-sensor is the substrate for the phosphotransferase reaction, whereas dephospho-sensor catalyzes the phosphatase reaction. Thus, higher levels of phospho-NarQ relative to phospho-NarX under these reaction conditions would lead to increased levels of phospho-His_6-NarL. Further analysis of phosphatase reactions will be reported elsewhere (C. E. Noriega. L.-L. Chen & V. Stewart, manuscript in preparation).

Overall, these results support the view that NarX and NarQ embody similar phosphoryl-transfer activities with NarL as substrate. Does this mean that each is as effective as the other at controlling NarL phosphorylation state in the wild-type? Probably not. For one thing, in cultures grown with nitrite (which stimulates NarQ but not NarX autophosphorylation), NarX phosphatase activity more than counterbalances NarQ phosphotransfer activity in order to enforce low levels of NarL-dependent gene expression (Rabin and Stewart, 1993; Stewart et al., 2002). For another, *narXL* operon expression is positively autoregulated, whereas expression of the *narQ* and *narP* genes is unregulated (Darwin and Stewart, 1995b), raising the likelihood that different protein concentrations *in vivo* result in different relative reaction rates.

NarX and NarQ act differentially to control NarP phosphorylation

Phosphoryl-transfer reactions involving NarP have been studied previously only as part of a global-scale study (Yamamoto *et al*., 2005). Here, MBP-NarQ was distinctly more effective than MBP-NarX at catalyzing His_6-NarP phosphorylation and dephosphorylation (Figs. 2B & D). Moreover, certain missense substitutions in the NarX DHp domain virtually eliminated phosphotransfer to NarP despite having little effect on phosphotransfer to NarL (Table 1; Fig. 6). Thus, unlike NarQ, NarX has greater preference for its cognate partner (NarL) than for its cross regulation partner (NarP). Accordingly, the core interaction network can now be depicted as asymmetric to reflect these differences (Fig. 1).

As noted above, analysis of NarQ and NarX relative involvement in mediating NarP-dependent gene expression *in vivo* has been hampered by technical limitations. The most recent study, employing a synthetic NarL and NarP transcriptional target, noted in passing that NarX appeared to be less effective than NarQ as a regulator of NarP phosphorylation (Stewart and Bledsoe, 2003).

Specificity in sensor-regulator interaction

Analyses to compare cognate vs. non-cognate interactions reveal strong preferences for the former, with phosphotransfer kinetic preference in the range of 10^4- to 10^5-fold for even closely-related pairs such as EnvZ-OmpR and CpxA-CpxR (Fisher et al., 1996; Skerker et al., 2008; Groban et al., 2009). Results presented here are in striking contrast. NarQ exhibited little if any preference for its cognate partner NarP over the non-cognate NarL, whereas NarX demonstrated only a modest preference, on the order of tenfold. Indeed, compared to other non-cognate interactions studied in detail (Fisher et al., 1996; Silva et al., 1998; Siryaporn and Goulian, 2008; Skerker et al., 2008; Groban et al., 2009), MBP-NarX phosphotransfer to His_6-NarP was remarkably efficient both *in vitro* (Figs. 2B & 3B) and *in vivo* (Table 1).

Previous studies with the EnvZ and NtrB sensors identified missense substitutions in both the DHp and CA domains that affect transmitter phosphatase activity (Atkinson and Ninfa, 1992; Hsing et al., 1998; Pioszak and Ninfa, 2003). Among a collection of NarX mutants that confer phenotypes resulting from defective transmitter phosphatase activity, a few (5 of 21) unexpectedly also conferred the striking NarP-blind phenotype (Table 1; Fig. 6). All of the NarP-blind alterations lie in the four-helix bundle that comprises the DHp domain (Dutta

et al., 1999; Gao and Stock, 2009). Other alterations within this region do not confer the NarP-blind phenotype, including other substitutions at two residues (Met-411 and Trp-442) defined also by NarP-blind mutants. Therefore, these mutants form a distinct class that interfere specifically with phosphotransfer to NarP but not to NarL. Strikingly, substitution directed to the corresponding residues in NarQ failed to identify a class of "NarL-blind" mutants (Table 5). Overall, the NarP-blind mutants confirm the observations summarized above, that NarX interacts more strongly with NarL than with NarP, because interaction with NarP was selectively lost by mutation.

Specificity determinants for sensor-regulator interaction have been identified by sequence, mutational and structural analyses to lie within a distinct region of the DHp domain, in the H box helix (but beyond the H box element itself), the X box helix, and the loop that connects the two. (Skerker et al., 2008; Szurmant et al., 2008; Casino et al., 2009). Strikingly, the corresponding sequence is different between the NarX and NarQ DHp domains (Fig. 7). Moreover, two of the positions defined by the NarP-blind mutants (Lys-410 and Met-411) correspond exactly to two positions identified elsewhere as contributing to sensor-regulator specificity (e.g., EnvZ Leu-254 and Ala-255, and TM0853 Ala-271 and Tyr-272) (Skerker et al., 2008; Szurmant et al., 2008).

X-ray structures for the *Bacillus subtilus* DesK transmitter were reported recently (Albanesi et al., 2009). The structure for unphosphorylated DesK displays the DHp domain as a four helix antiparallel coiled-coil, including the characteristic heptad repeat pattern of nonpolar residues (reviewed by (Lupas and Gruber, 2005). The DesK, NarX and NarQ transmitters are in the distinct HPK7 sequence subfamily (Grebe and Stock, 1999; Wolanin et al., 2002), the DHp sequence of which is denoted also as HisKA_3 (pfam00730; (Finn et al., 2008). Fig. 7 shows the heptad repeats from the unphosphorylated DesK structure mapped onto the corresponding positions within NarX and NarQ. The two α-helices extend beyond the limits of the H box and X box sequence motifs, and so all DHp substitutions reported here lie in one or the other helix (Fig. 7). Most are at surface-exposed positions, as expected for residues involved in protein-protein interactions.

Structural analysis indicates that residues within both the H box and X box helices engage in direct protein-protein interaction with the receiver domain (Casino et al., 2009). Thus, residues in the X box helix likely also contribute to specificity (Skerker et al., 2008; Szurmant et al., 2008); NarX residue Trp-442 is so identified in this study. By contrast, NarX residue Phe-452 lies in a region of extensive sequence identity between NarX and NarQ (Fig. 7) and therefore seems a less-likely candidate for mediating receiver interaction specificity. However, the F452Y mutant uniquely exhibited yet another unexpected phenotype, ADP-insensitive autophosphorylation (Fig. 5). Moreover, residue Phe-452 occupies a heptad repeat "a" position and therefore lies within the interior of the DHp coiled-coil as deduced from the DesK structure (Fig. 7) Thus, this alteration may manifest its NarP-blind phenotype through influence on transmitter activities rather than sensor-receiver interaction per se.

All examined nitrite-hypersensitive mutants have lost negative function, primarily a NarL-based phenotype. However, their NarP-based phenotypes can vary considerably (Williams and Stewart, 1997a, b); **this study**). Thus, although some overlap between NarX-NarL transmitter phosphatase activity and NarX-NarP transmitter phosphotransferase activity is demonstrated by substitutions that affect both processes, these two functions also are genetically separable. Reciprocal interactions would be mechanistically informative. Thus, one future challenge is to identify NarP-blind mutants that retain near-normal activities toward NarL.

Experimental procedures

Strains, plasmids and β-Galactosidase assay

Most *E. coli* strains and plasmids are described elsewhere in detail (Williams and Stewart, 1997a). NarL- abd NarP-dependent gene expression was analyzed in strains VJS5054 {Δ*narX narQ*::Tn*10* Φ(*narG-lacZ*) *pcnB1*} and VJS5721 {Δ(*narXL*) *narQ*::Tn*10* Φ(*napF-lacZ*) *pcnB1*}, respectively. Negative function, representing phospho-NarL phosphatase activity, was analyzed in strain VJS5720 {Δ*narX narQ*::Tn*10 narL505* Φ(*narG-lacZ*) *pcnB1*}. The *narL* null allele in this strain eliminates phospho-NarL antagonism of *napF* operon expression (Darwin and Stewart, 1995a). Transmitter kinase activity was assessed in strain VJS5768 {λΦ(*frdA-lacZ*)Δ*narX242 narQ251*::Tn*10*d(Tc) *pcnB1 zad-981*::Tn*10*d(Km)}, which was derived by transducing the *pcnB1 zad-981*::Tn*10*d(Km) region into strain VJS3046 (Rabin and Stewart, 1993). The *pcnB1* allele (Liu and Parkinson, 1989) was used to mimic single-copy status for plasmid-borne *narX* alleles (Williams and Stewart, 1997a).

Plasmid pVJS1241 carries the $narX^{\dagger}$ allele containing silent restriction endonuclease sites introduced to facilitate recloning of defined segments (Williams and Stewart, 1997a). A few experiments used plasmid pVJS2474 carrying the $narX^{\ddagger}$ allele, a derivative that contains additional unique sites (Appleman and Stewart, 2003). These silent restriction sites permit recloning of relatively small segments into otherwise unmutagenized plasmid backgrounds, in order to minimize the occurance of spurious mutational changes.

Plasmid pVJS1231 carries the $narQ^{+}$ gene (Williams and Stewart, 1997a). The two native *Nru*I sites, centered at codons Arg-275 (in the central module) and Arg-475 (in the CA domain N box element), were used to reclone the intervening segment following site-specific mutagenesis.

β-Galactosidase activity was measured from cultures grown anaerobically in MOPS defined medium (Stewart and Parales, 1988). $NaNO_3$ (40 mM), $NaNO_2$ (5 mM) and ampicillin (50 μg^{-1} ml) were added as indicated. All cultures were assayed in duplicate, and the reported values are averages from at least two independent experiments. Specific activities are expressed in arbitary units (Miller, 1972).

Mutant isolation and characterization

Missense alterations in the *narX* gene were isolated by error-prone polymerase chain reaction (PCR) mutagenesis followed by phenotypic screening as described previously in detail (Williams and Stewart, 1997a). Mutagenesis was directed to NarX codons Arg-195 through Pro-349 (a 460 nt *Nru*I-*Eco*NI fragment spanning the middle of the HAMP domain through much of the central module); codons Pro-349 through Ala-440 (a 270 nt *Eco*NI-*Nsi*I fragment spanning the rest of the central module through the middle of the transmitter X box element); and codons Ala-440 through Glu-598 (a 650 nt *Nsi*I-*Bgl*II fragment encoding the remainder of the transmitter module).

Oligonucleotde-directed site-specific mutagenesis was performed as described previously (Appleman and Stewart, 2003) to revert the NarX Q412R and V413M alterations separately, and to make the NarQ R381E, Y413R and F423Y substitutions (Table 5). Random alterations at NarQ codons Arg-381 and Ile-382 were made by using oligonucleotides in which the indicated codons were synthesized with equal amounts of all four nucleotides (Table 5) (Hermes et al., 1989). Mutant phenotypes were identified by screening colonies on MacConkey medium (Williams and Stewart, 1997a). Several colonies with wild-type phenotypes were evaluated also, to ensure that the mutagenesis protocol had generated a range of alterations at the desired codons.

All mutational alterations were identified by sequencing both strands from the region recloned into unmutagenized parent plasmid. DNA sequencing was performed by the dideoxy chain termination method as described previously (Williams and Stewart, 1997a; Pope et al., 2009).

Molecular cloning

Standard methods were used for restriction endonuclease digestion, ligation, transformation, and PCR amplification of DNA (Maloy et al., 1996). All MBP and His_6 expression plasmids were introduced into *E. coli* host strains JM109 (Yanisch-Perron et al., 1985) and M15 (Qiagen, Valencia, CA), respectively. Plasmids expressing MBP-NarX and MBP-NarQ were constructed by PCR using oligonucleotide primers (Table 5), containing *Xba*I and *Hind*III sites, which were used to clone the constructs into the *Xba*I and *Hind*III sites of plasmid pMAL-c (New England Biolabs, Beverly, MA).

The MBP-NarP fusion was described previously (Darwin and Stewart, 1995a). Plasmids expressing His_6-NarL and His_6-NarP were constructed by PCR using the $narL^+$ and $narP^+$ alleles, respectively. For NarL, the His_6-tag was fused spanning codons 2–3 ($MRGSH_6G$*SNQ*…), and for NarP, spanning codons 1–2 ($MRGSH_6GI$*PE*…) (italics designate the start of NarL or NarP residues). Oligonucleotide primers (Table 5), containing *BamH*I and *Hind*III sites, were used to clone the constructs into the *BamH*I and *Hind*III sites of plasmids pQE30 ($narL^+$) or pQE32 ($narP^+$) (Qiagen).

Overexpression and protein enrichment

Bacterial strains were cultured at 37°C in Tryptone-Yeast extract (TY) broth (tryptone 8 g L^{-1}, yeast extract 5 g L^{-1}, NaCl 5 g L^{-1}) with shaking at 200 rpm. For plasmid selection, TY broth was supplemented with ampicillin (100 μg ml^{-1}).

MBP-Nar sensor proteins were isolated as described previously (Noriega et al., 2008) with the following modifications. MBP-NarX and MBP-NarQ were enriched from 1 L culture volumes using a 25 ml column containing 10 ml amylose resin. Proteins were collected in 20 mM HEPES pH 7.0, 200 mM KCl, 1 mM dithiothreitol (DTT), 5 % (vol/vol) glycerol, 1 mM phenylmethanesulfonylfluoride (PMSF) and 10 mM maltose typically as four peak 1 ml fractions. Both soluble and particulate fractions from crude extracts of all MBP-Nar-sensor overexpression cultures were monitored. The MBP-Nar-sensor proteins partitioned approximately equally between the two.

For size exclusion chromatography, peak elution fractions of MBP-NarX and MBP-NarQ from affinity chromatography described above were pooled and concentrated using Vivaspin 6 (VWR, West Chester, PA). Typically, 4 ml of eluted protein was concentrated to an approximate volume of 0.5 ml (30–50 mg ml^{-1}). 250 μl of concentrated preparations were loaded on a Sephacryl S-200, HR 10/30 (GE Healthcare, Piscataway, NJ), equilibrated with 20 mM HEPES pH 7.0, 200 mM KCl, 1 mM DTT, and 5% v/v glycerol. The column was run at 0.25 ml min^{-1}. Protein was collected by monitoring absorption at 280 nm. Elution profiles indicate both proteins were predominately dimers according to their calculated molecular mass (MBP-NarX, 170 kDa and MBP-NarQ, 164 kDa). Furthermore, both autophosphorylation as well as phosphoryl transfer reactions were relatively unaffected when comparing activities of affinity-enriched MBP-sensor preparations before and after size exclusion chromatography (**data not shown**). As alluded previously (Noriega et al., 2008), most protein became insoluble upon factor Xa proteolytic separation from MBP (**data not shown**).

Strains expressing His_6-NarP consistently produced less soluble protein compared with His_6-NarL. To obtain comparable protein concentrations, strains expressing His_6-NarL and

His_6-NarP were inoculated in 250 ml and 1 L culture volumes respectively. Expression was induced with 0.5 mM IPTG during exponential phase (approximately 80 Klett units) and incubation continued for 2.5 h. All procedures thereafter were performed at 4°C. Cells were harvested by centrifugation at 10,000 × g for 10 min. Pellets were washed with suspension buffer consisting of 20 mM sodium phosphate pH 7.4, 500 mM KCl, 50 mM imidazole and 5% v/v glycerol, and resuspended in the same buffer supplemented with 1 mM PMSF. Cell suspensions were disrupted by passage through a French pressure cell at 20,000 psi. Soluble and particulate fractions were separated by centrifugation at 20,000 × g for 30 min. The soluble fraction was subjected to affinity chromatography using a 1 ml HisTrap HP column (GE Healthcare, Piscataway, NJ) pre-equilibrated with suspension buffer. The column was washed with 5 ml suspension buffer and eluted with 5 ml of the same buffer supplemented with 500 mM imidazole. Peak elution fractions were typically collected as two separate 0.5 ml fractions.

Dialysis of His_6-NarL and His_6-NarP preparations was performed to remove imidazole. To minimize precipitation, buffer exchange was performed by four successive dialysis steps at 4°C using Slide-A-Lyzer (Pierce, Rockford, IL). Proteins were first dialyzed against 20 mM HEPES pH 7.0, 1 M KCl and 5% v/v glycerol for 2 h. This was repeated two additional times in the same buffer but with decreasing KCl concentrations of 750 mM and 500 mM respectively. The final dialysis step was performed overnight against the same buffer with 250 mM KCl and 10% v/v glycerol. Approximately 10% of the dialyzed protein was lost to precipitation. The soluble fractions were collected by centrifugation at 16,000 × g for 10 min. Enrichment of MBP-NarP was performed as described previously (Darwin and Stewart, 1995a).

Protein preparations were evaluated by electrophoresis through denaturing slab gels (Laemmli, 1970) which were stained with SYPRO Ruby Protein Stain (Bio-Rad, Hercules, CA) and visualized with a FluorChem imaging system (Alpha Innotech, San Leandro, CA). All protein preparations were highly enriched, with only trace amounts of contaminating species apparent (**data not shown**). Proteins were stored at −80°C as frozen aliquots from dry ice ethanol exposure. Final protein concentrations (as monomers) were determined by measuring absorbance at 280 nm. All chemicals and reagents were from Sigma-Aldrich Corp. (St. Louis, MO) except as noted.

Nucleotides

[γ-^{32}P]ATP (10 mCi ml^{-1}, 3000 Ci mmol^{-1}, PerkinElmer, Waltham, MA), ATP and ADP (Sigma-Aldrich Corp., cat. A-2383 and cat. A-2754 respectively) were ≥ 98% pure as indicated by the manufacturers.

Autophosphorylation

Buffer for all reactions contained 100 mM HEPES pH 7.0, 50 mM KCl, 12.5 mM $MgCl_2$, 12.5 mM $MnCl_2$, 2.5 mM DTT and 10% glycerol. This is the same buffer described previously (Noriega et al., 2008), except that DTT concentration was decreased from 10 mM to 2.5 mM, which had no observable effect on autophosphorylation rates. Concentrations of $MgCl_2$ and $MnCl_2$ were erroneously reported as 5 mM each (Noriega et al., 2008); the actual concentrations (12.5 mM each) were also used in the experiments reported here.

Autophosphorylation and dephosphorylation reactions of MBP-Nar sensors were performed at 19°C essentially as described (Noriega et al., 2008). Instead of 2.5 μM dimers of MBP-Nar sensor (12.5 pmol total per reaction), only 0.5 μM dimers MBP-Nar sensor protein (2.5 pmol total per reaction) was used. Where indicated, reactions were supplemented with ATP-regeneration as described previously (Noriega et al., 2008). All autophosphorylation

reactions were measured from 5 μl time-point samples with 100μM [γ-^{32}P] ATP except as noted.

The MBP-NarX and MBP-NarQ proteins used here have slightly different junction points from those described previously (Noriega et al., 2008). In order to compare their properties, we examined their autophosphorylation and dephosphorylation kinetics (Noriega et al., 2008). Dephosphorylation rates, as well as affinities for both ATP and ADP, were virtually indistinguishable from those previously determined (**data not shown**). However, autophosphorylation rates were approximately 16-fold faster than those previously determined. This was due to the higher specific activity for the proteins used here: in reactions containing ATP-regeneration, we observed substantially higher autophosphorylation levels approaching 100 % in some experiments (**data not shown**), presuming that sensor dimers are predominately hemiphosphorylated (Jiang et al., 2000). Gel filtration did not affect autophosphorylation rates or levels (**data not shown**).

Phosphoryl-transfer

Phosphorylated MBP-Nar sensor was obtained from reactions containing 0.5 μM dimers of MBP-Nar sensor incubated for 45–90 min with ATP-regeneration as described above. Phospho-MBP-Nar sensor devoid of nucleotides was isolated with Vivaspin 500 (VWR, West Chester, PA) as described previously (Noriega et al., 2008). Phosphoryl transfer reactions were initiated by the addition of His_6-Nar response regulator(s) to a final concentration of 10 μM monomers to the autophosphorylation reaction cocktail containing phosphorylated MBP-Nar sensor with 100 μM [γ-^{32}P]ATP and ATP-regeneration (multiple-round reactions) or to phospho-MBP-sensor devoid of nucleotides (single-round reactions). Phosphoryl-transfer reactions were performed at 19°C or 4°C (MiniFridge II, Boekel Scientific, Feasterville, PA) as indicated in the text. Reaction samples (5 μl) were withdrawn at indicated time intervals, mixed with equal volume of 2X protein loading buffer containing 0.5 M Tris-HCl pH 6.8, 4.4% (w/v) SDS, 20% (v/v) glycerol, 2% (v/v) β-mercaptoethanol and bromophenol blue, and loaded onto 12% Laemmli gels. Following electrophoresis, the gels were dried and exposed to a phosphorimage screen for quantification as described below.

Quantification of phosphorylated protein

MBP-Nar sensor autophosphorylation was quantified by filter binding as described previously (Noriega et al., 2008). Phosphoryl-transfer from sensor to regulator was quantified by preparing a standard curve. Serial dilutions from the reaction mixtures were transferred onto Whatman blotting paper grade 3MM Chr (GE Healthcare, Piscataway, NJ) as 5 μl spots, dried, and exposed to a phosphorimage screen simultaneously with the Laemmli gel(s) containing the phosphoryl-transfer reactions mentioned above. Band and spot intensities of the gel(s) and blotting paper respectively, were analyzed using a Storm Scanner with ImageQuant Software (Molecular Dynamics, Cupertino, CA). Each spot from the blotting paper was then cut and counted by liquid scintillation (Ready Protein, Beckman Coulter, Fullerton, CA).

Estimated kinetic preferences for phosphotransferase reactions

Initial velocities (V_0) were estimated from single-round phosphoryl-transfer time-course reactions, similar to those described previously (Skerker et al., 2005; Skerker et al., 2008). Data were collected as a single time point sample (5 μl) at 60 s for MBP-NarX plus His_6-NarP, and at 15 s for all other pairwise combinations. Reactions contained 0.5 μM (dimers) of MBP-Nar sensor and 1 μM (monomers) of His_6-Nar response regulator. These parameters were chosen from an extensive series of measurements made initially with the goal of determining Michaelis-Menten constants. Estimated values for V_0 were calculated by

dividing the amount of accumulated phospho-regulator by the initial amount of phospho-sensor. Values are averaged from three independent determinations performed on different days. Relative kinetic preference was determined from the ratio of cognate to non-cognate V_0 values (Skerker et al., 2005).

Reproducibility of results

Independent phosphoryl-transfer reactions were initiated with different amounts of phosphorylated sensor, due to variability in accumulation on different days with different protein preparations and lots of radiolabel. Because of this, meaningful standard errors cannot be calculated for a series of replicate experiments. Accordingly, results depicted in Figs. 2–6 are from representative individual experiments.

Overall results are supported qualitatively by dozens of experiments, conducted over several years by different investigators using different protein preparations and reaction conditions. Results summarized in Figs. 2–6 are representative of duplicate (or triplicate in the case of Fig. 6) experiments conducted under essentially identical conditions that differed, if at all, only in the lot of radiolabel used.

Acknowledgments

We are especially grateful to Juan Parales for his invaluable assistance and advice with size-exclusion chromatography and other protein enrichment procedures. Drs. Gwénola Simon and J. Alex Appleman made important contributions with their preliminary analyses of phosphoryl-transfer reactions, and Dr. Alice Lin provided much-needed help with His_6-Nar regulator enrichment and dialysis. We thank Jiarong Shi for fabricating the His_6-Nar regulator constructs, Prof. Becky Parales for use of her FPLC apparatus, and Prof. Andrew Darwin for suggesting the *in vivo* test to monitor strength of NarX transmitter phosphotransferase activity.

This study was supported by U. S. Public Health Service Grant GM036877 from the National Institute of General Medical Sciences.

References

Albanesi D, Martin M, Trajtenberg F, Mansilla MC, Haouz A, Alzari PM, et al. Structural plasticity and catalysis regulation of a thermosensor histidine kinase. Proc Natl Acad Sci USA. 2009; 106:16185–16190. [PubMed: 19805278]

Alves R, Savageau MA. Comparative analysis of prototype two-component systems with either bifunctional or monofunctional sensors: differences in molecular structure and physiological function. Mol Microbiol. 2003; 48:25–51. [PubMed: 12657043]

Appleman JA, Stewart V. Mutational analysis of a conserved signal-transducing element: the HAMP linker of the *Escherichia coli* nitrate sensor NarX. J Bacteriol. 2003; 185:89–97. [PubMed: 12486044]

Atkinson MR, Ninfa AJ. Characterization of Escherichia coli *glnL* mutations affecting nitrogen regulation. J Bacteriol. 1992; 174:4538–4548. [PubMed: 1352516]

Cai SJ, Inouye M. EnvZ-OmpR interaction and osmoregulation in *Escherichia coli*. J Biol Chem. 2002; 277:24155–24161. [PubMed: 11973328]

Casino P, Rubio V, Marina A. Structural insight into partner specificity and phosphoryl transfer in two-component signal transduction. Cell. 2009; 139:325–336. [PubMed: 19800110]

Cavicchioli R, Schröder I, Constanti M, Gunsalus RP. The NarX and NarQ sensor-transmitter proteins of *Escherichia coli* each require two conserved histidines for nitrate-dependent signal transduction to NarL. J Bacteriol. 1995; 177:2416–2424. [PubMed: 7730273]

Chiang RC, Cavicchioli R, Gunsalus RP. Identification and characterization of *narQ*, a second nitrate sensor for nitrate-dependent gene regulation in *Escherichia coli*. Mol Microbiol. 1992; 6:1913–1923. [PubMed: 1508040]

Darwin AJ, Stewart V. Nitrate and nitrite regulation of the Fnr-dependent *aeg-46.5* promoter of *Escherichia coli* K-12 is mediated by competition between homologous response regulators (NarL and NarP) for a common DNA-binding site. J Mol Biol. 1995a; 251:15–29. [PubMed: 7643383]

Darwin AJ, Stewart V. Expression of the *narX*, *narL*, *narP*, and *narQ* genes of *Escherichia coli* K-12: regulation of the regulators. J Bacteriol. 1995b; 177:3865–3869. [PubMed: 7601854]

Dutta R, Qin L, Inouye M. Histidine kinases: diversity of domain organization. Mol Microbiol. 1999; 34:633–640. [PubMed: 10564504]

Egan SM, Stewart V. Nitrate regulation of anaerobic respiratory gene expression in *narX* deletion mutants of *Escherichia coli* K-12. J Bacteriol. 1990; 172:5020–5029. [PubMed: 2144276]

Egan SM, Stewart V. Mutational analysis of nitrate regulatory gene *narL* in *Escherichia coli* K-12. J Bacteriol. 1991; 173:4424–4432. [PubMed: 2066339]

Finn RD, Tate J, Mistry J, Coggill PC, Sammut SJ, Hotz HR, et al. The Pfam protein families database. Nucleic Acids Res. 2008; 36:D281–288. [PubMed: 18039703]

Fisher SL, Kim SK, Wanner BL, Walsh CT. Kinetic comparison of the specificity of the vancomycin resistance VanS for two response regulators, VanR and PhoB. Biochemistry. 1996; 35:4732–4740. [PubMed: 8664263]

Gao R, Stock AM. Biological insights from structures of two-component proteins. Annu Rev Microbiol. 2009; 63:133–154. [PubMed: 19575571]

Gennis, RB.; Stewart, V. Respiration. In: Neidhardt, FC.; Curtiss, R., III; Ingraham, JL.; Lin, ECC.; Low, KB.; Magasanik, B.; Reznikoff, WS.; Riley, M.; Schaechter, M.; Umbarger, HE., editors. Escherichia coli and Salmonella Cellular and Molecular Biology. Washington, D. C: ASM Press; 1996. p. 217-261.

Grebe TW, Stock JB. The histidine kinase superfamily. Adv Microbial Physiol. 1999; 41:139–227.

Groban ES, Clarke EJ, Salis HM, Miller SM, Voigt CA. Kinetic buffering of cross talk between bacterial two-component sensors. J Mol Biol. 2009; 390:380–393. [PubMed: 19445950]

Hermes JD, Parekh SM, Blacklow SC, Koster H, Knowles JR. A reliable method for random mutagenesis: the generation of mutant libraries using spiked oligodeoxyribonucleotide primers. Gene. 1989; 84:143–151. [PubMed: 2691332]

Hoch JA, Varughese KI. Keeping signals straight in phosphorelay signal transduction. J Bacteriol. 2001; 183:4941–4949. [PubMed: 11489844]

Hsing W, Russo FD, Bernd KK, Silhavy TJ. Mutations that alter the kinase and phosphatase activities of the two-component sensor EnvZ. J Bacteriol. 1998; 180:4538–4546. [PubMed: 9721293]

Igo MM, Ninfa AJ, Silhavy TJ. A bacterial environmental sensor that functions as a protein kinase and stimulates transcriptional activation. Genes Dev. 1989; 3:598–605. [PubMed: 2663643]

Janiak-Spens F, Cook PF, West AH. Kinetic analysis of YPD1-dependent phosphotransfer reactions in the yeast osmoregulatory phosphorelay system. Biochemistry. 2005; 44:377–386. [PubMed: 15628880]

Jiang M, Tzeng YL, Feher VA, Perego M, Hoch JA. Alanine mutants of the Spo0F response regulator modifying specificity for sensor kinases in sporulation initiation. Mol Microbiol. 1999; 33:389–395. [PubMed: 10411754]

Jiang P, Peliska JA, Ninfa AJ. Asymmetry in the autophosphorylation of the two-component regulatory system transmitter protein nitrogen regulator II of *Escherichia coli*. Biochemistry. 2000; 39:5057–5065. [PubMed: 10819971]

Kiil K, Ferchaud JB, David C, Binnewies TT, Wu H, Sicheritz-Ponten T, et al. Genome update: distribution of two-component transduction systems in 250 bacterial genomes. Microbiology. 2005; 151:3447–3452. [PubMed: 16272367]

Laemmli UK. Cleavage of structural proteins during the assembly of the head of bacteriophage T4. Nature. 1970; 227:680–685. [PubMed: 5432063]

Laub MT, Goulian M. Specificity in two-component signal transduction pathways. Annu Rev Genet. 2007; 41:121–145. [PubMed: 18076326]

Lee AI, Delgado A, Gunsalus RP. Signal-dependent phosphorylation of the membrane-bound NarX two-component sensor-transmitter protein of *Escherichia coli*: nitrate elicits a superior anion ligand response compared to nitrite. J Bacteriol. 1999; 181:5309–5316. [PubMed: 10464202]

Li J, Kustu S, Stewart V. In vitro interaction of nitrate-responsive regulatory protein NarL with DNA target sequences in the *fdnG*, *narG*, *narK* and *frdA* operon control regions of *Escherichia coli* K-12. J Mol Biol. 1994; 241:150–165. [PubMed: 8057356]

Liu J, Parkinson JS. Genetics and sequence analysis of the *pcnB* locus, an *Escherichia coli* gene involved in plasmid copy number control. J Bacteriol. 1989; 171:1254–1261. [PubMed: 2537812]

Lupas AN, Gruber M. The structure of α-helical coiled coils. Adv Protein Chem. 2005; 70:37–78. [PubMed: 15837513]

Maloy, SR.; Stewart, VJ.; Taylor, RK. Genetic analysis of pathogeneic bacteria. A laboratory manual. Cold Spring Harbor, N. Y: Cold Spring Harbor Laboratory Press; 1996.

Mattison K, Kenney LJ. Phosphorylation alters the interaction of the response regulator OmpR with its sensor kinase EnvZ. J Biol Chem. 2002; 277:11143–11148. [PubMed: 11799122]

Miller, JH. Experiments in molecular genetics. Cold Spring Harbor Laboratory; Cold Spring Harbor, N Y: 1972.

Ninfa AJ, Magasanik B. Covalent modification of the *glnG* product, NRI, by the *glnL* product, NRII, regulates the transcription of the *glnALG* operon in *Escherichia coli*. Proc Natl Acad Sci USA. 1986; 83:5909–5913. [PubMed: 2874557]

Ninfa AJ, Ninfa EG, Lupas AN, Stock A, Magasanik B, Stock J. Crosstalk between bacterial chemotaxis signal transduction proteins and regulators of transcription of the Ntr regulon: evidence that nitrogen assimilation and chemotaxis are controlled by a common phosphotransfer mechanism. Proc Natl Acad Sci USA. 1988; 85:5492–5496. [PubMed: 3041412]

Ninfa, AJ.; Atknison, MR.; Kamberov, ES.; Feng, J.; Ninfa, EG. Control of nitrogen assimilation by the NR_I-NR_{II} two-component system of enteric bacteria. In: Hoch, JA.; Silhavy, TJ., editors. Two-component signal transduction. Washington D. C: ASM Press; 1995. p. 67-88.

Noriega CE, Schmidt R, Gray MJ, Chen LL, Stewart V. Autophosphorylation and dephosphorylation by soluble forms of the nitrate-responsive sensors NarX and NarQ from *Escherichia coli* K-12. J Bacteriol. 2008; 190:3869–3876. [PubMed: 18375557]

Parkinson JS, Kofoid EC. Communication modules in bacterial signaling proteins. Annu Rev Genet. 1992; 26:71–112. [PubMed: 1482126]

Pioszak AA, Ninfa AJ. Genetic and biochemical analysis of phosphatase activity of *Escherichia coli* NRII (NtrB) and its regulation by the PII signal transduction protein. J Bacteriol. 2003; 185:1299–1315. [PubMed: 12562801]

Pope SD, Chen LL, Stewart V. Purine utilization by *Klebsiella oxytoca* M5al: genes for ring-oxidizing and -opening enzymes. J Bacteriol. 2009; 191:1006–1017. [PubMed: 19060149]

Pratt, LA.; Silhavy, TJ. Porin regulon of *Escherichia coli*. In: Hoch, JA.; Silhavy, TJ., editors. Two-component signal transduction. Washington D. C: ASM Press; 1995. p. 105-127.

Price MN, Dehal PS, Arkin AP. Horizontal gene transfer and the evolution of transcriptional regulation in *Escherichia coli*. Genome Biol. 2008; 9:R4. [PubMed: 18179685]

Rabin RS, Stewart V. Either of two functionally redundant sensor proteins, NarX and NarQ, is sufficient for nitrate regulation in *Escherichia coli* K-12. Proc Natl Acad Sci USA. 1992; 89:8419–8423. [PubMed: 1528845]

Rabin RS, Stewart V. Dual response regulators (NarL and NarP) interact with dual sensors (NarX and NarQ) to control nitrate- and nitrite-regulated gene expression in *Escherichia coli* K-12. J Bacteriol. 1993; 175:3259–3268. [PubMed: 8501030]

Schröder I, Wolin CD, Cavicchioli R, Gunsalus RP. Phosphorylation and dephosphorylation of the NarQ, NarX, and NarL proteins of the nitrate-dependent two-component regulatory system of *Escherichia coli*. J Bacteriol. 1994; 176:4985–4992. [PubMed: 8051011]

Silva JC, Haldimann A, Prahalad MK, Walsh CT, Wanner BL. *In vivo* characterization of the type A and B vancomycin-resistant enterococci (VRE) VanRS two-component systems in *Escherichia coli*: a nonpathogenic model for studying the VRE signal transduction pathways. Proc Natl Acad Sci USA. 1998; 95:11951–11956. [PubMed: 9751771]

Siryaporn A, Goulian M. Cross-talk suppression between the CpxA-CpxR and EnvZ-OmpR two-component systems in *E. coli*. Mol Microbiol. 2008; 70:494–506. [PubMed: 18761686]

Skerker JM, Prasol MS, Perchuk BS, Biondi EG, Laub MT. Two-component signal transduction pathways regulating growth and cell cycle progression in a bacterium: a system-level analysis. PLoS Biol. 2005; 3:e334. [PubMed: 16176121]

Skerker JM, Perchuk BS, Siryaporn A, Lubin EA, Ashenberg O, Goulian M, Laub MT. Rewiring the specificity of two-component signal transduction systems. Cell. 2008; 133:1043–1054. [PubMed: 18555780]

Stewart V, Parales J Jr. Identification and expression of genes *narL* and *narX* of the *nar* (nitrate reductase) locus in *Escherichia coli* K-12. J Bacteriol. 1988; 170:1589–1597. [PubMed: 2832370]

Stewart, V.; Rabin, RS. Dual sensors and dual response regulators interact to control nitrate- and nitrite-responsive gene expression in *Escherichia coli*. In: Hoch, JA.; Silhavy, TJ., editors. Two-component signal transduction. Washington D. C: ASM Press; 1995. p. 233-252.

Stewart V, Lu Y, Darwin AJ. Periplasmic nitrate reductase (NapABC enzyme) supports anaerobic respiration by *Escherichia coli* K-12. J Bacteriol. 2002; 184:1314–1323. [PubMed: 11844760]

Stewart V. Nitrate- and nitrite-responsive sensors NarX and NarQ of proteobacteria. Biochem Soc Trans. 2003; 31:1–10. [PubMed: 12546643]

Stewart V, Bledsoe PJ. Synthetic *lac* operator substitutions to study the nitrate- and nitrite-responsive NarX-NarL and NarQ-NarP two-component regulatory systems of *Escherichia coli* K-12. J Bacteriol. 2003; 185:2104–2111. [PubMed: 12644479]

Stewart V, Chen LL, Wu HC. Response to culture aeration mediated by the nitrate and nitrite sensor NarQ of *Escherichia coli* K-12. Mol Microbiol. 2003; 50:1391–1399. [PubMed: 14622424]

Stock AM, Robinson VL, Goudreau PN. Two-component signal transduction. Annu Rev Biochem. 2000; 69:183–215. [PubMed: 10966457]

Stock, JB.; Surette, MG.; Levit, M.; Park, P. Two-component signal transduction systems: structure-function relationships and mechanisms of catalysis. In: Hoch, JA.; Silhavy, TJ., editors. Two-component signal transduction. Washington D. C: ASM Press; 1995. p. 25-51.

Szurmant H, Bobay BG, White RA, Sullivan DM, Thompson RJ, Hwa T, et al. Co-evolving motions at protein-protein interfaces of two-component signaling systems identified by covariance analysis. Biochemistry. 2008; 47:7782–7784. [PubMed: 18588317]

Walker MS, DeMoss JA. Phosphorylation and dephosphorylation catalyzed in vitro by purified components of the nitrate sensing system, NarX and NarL. J Biol Chem. 1993; 268:8391–8393. [PubMed: 8473280]

Wanner BL. Is cross regulation by phosphorylation of two-component response regulator proteins important in bacteria? J Bacteriol. 1992; 174:2053–2058. [PubMed: 1551826]

Wanner, BL.; Jiang, W.; Kim, S-K.; Yamagata, D.; Haldimann, A.; Daniels, LL. Are the multiple signal transduction pathways of the Pho regulon due to cross talk or cross regulation?. In: Lin, ECC.; Lynch, AS., editors. Regulation of gene expression in Escherichia coli. Georgetown, TX: R G Landes Co; 1996. p. 297-315.

Williams SB, Stewart V. Nitrate- and nitrite-sensing protein NarX of *Escherichia coli* K-12: mutational analysis of the amino-terminal tail and first transmembrane segment. J Bacteriol. 1997a; 179:721–729. [PubMed: 9006026]

Williams SB, Stewart V. Discrimination between structurally related ligands nitrate and nitrite controls autokinase activity of the NarX transmembrane signal transducer of *Escherichia coli* K-12. Mol Microbiol. 1997b; 26:911–925. [PubMed: 9426129]

Wolanin PM, Thomason PA, Stock JB. Histidine protein kinases: key signal transducers outside the animal kingdom. Genome Biol. 2002; 3:reviews3013.3011–3013.3018. [PubMed: 12372152]

Yamamoto K, Hirao K, Oshima T, Aiba H, Utsumi R, Ishihama A. Functional characterization *in vitro* of all two-component signal transduction systems from *Escherichia coli*. J Biol Chem. 2005; 280:1448–1456. [PubMed: 15522865]

Yanisch-Perron C, Vieira J, Messing J. Improved M13 phage cloning vectors and host strains: nucleotide sequences of the M13mp18 and pUC19 vectors. Gene. 1985; 33:103–119. [PubMed: 2985470]

Yoshida T, Cai S, Inouye M. Interaction of EnvZ, a sensory histidine kinase, with phosphorylated OmpR, the cognate response regulator. Mol Microbiol. 2002; 46:1283–1294. [PubMed: 12453215]

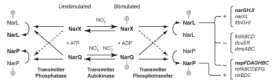

Fig. 1.

Model for asymmetry in the NarX-NarL and NarQ-NarP cross regulation network. Dashed arrows represent relatively slow reactions. The NarX and NarQ sensor populations are hypothesized to be in a two-state equilibrium determined by stimulus (ligand binding). Phospho-sensors catalyze response regulator phosphorylation, whereas dephospho-sensors catalyze regulator dephosphorylation. Phospho-regulators activate (+) or repress (−) transcription; representative target operons are shown.

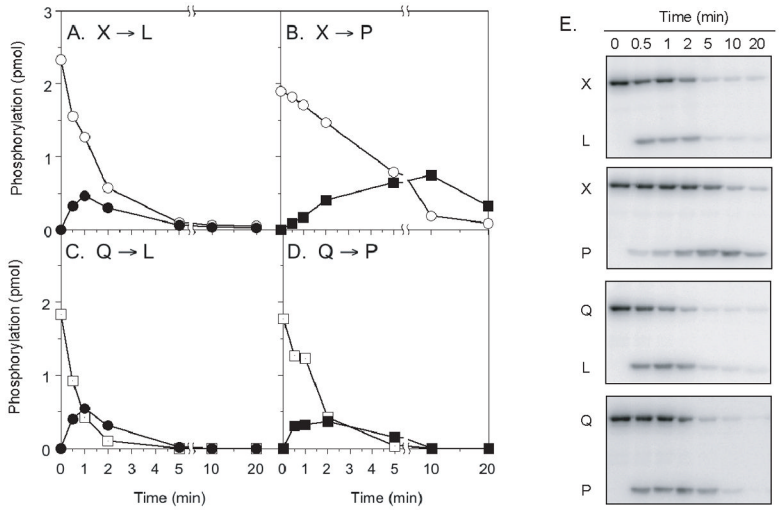

Fig. 2.

Single-round phosphoryl-transfer between Nar sensors and response regulators in the absence of nucleotides. ○, Phospho-MBP-NarX$_{227}$; □, phospho-MBP-NarQ$_{226}$; ●, phospho-His$_6$-NarL; ■, phospho-His$_6$-NarP. Sensors (0.5 μM dimers), prepared from gel-filtration, were incubated with ^{32}P-ATP for autophosphorylation, and then nucleotides were removed by filtration through a spin column. Response regulators (10 μM monomers) were added at time = 0, and time-point samples were resolved by Laemmli gel electrophoresis. Panels A-D show results for the indicated combinations. Panel E shows phosphorimages of the gels used for these plots.

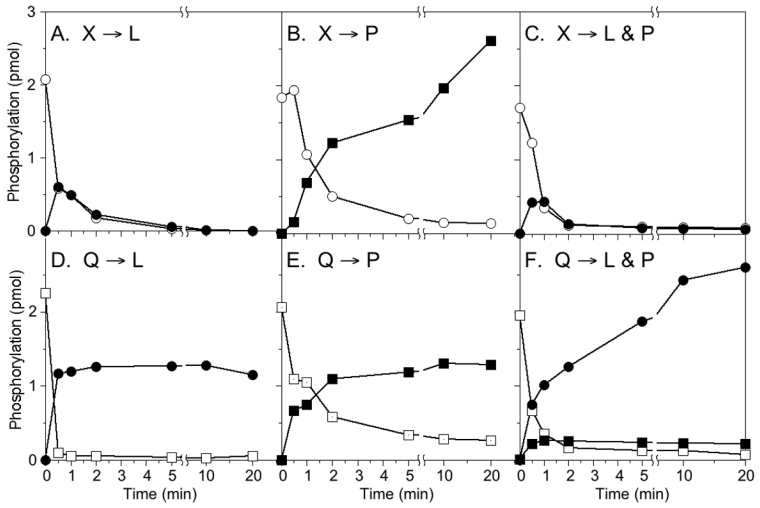

Fig. 3.

Multiple-round phosphoryl-transfer between Nar sensors and response regulators in the presence of nucleotides. Results are from a single representative experiment; others not shown generated similar patterns. ○, Phospho-MBP-NarX$_{227}$; □, phospho-MBP-NarQ$_{226}$; ●, phospho-His$_6$-NarL; ■, phospho-His$_6$-NarP. Sensors (0.5 μM dimers), prepared from gel filtration, were incubated with ^{32}P-ATP for autophosphorylation in the presence of ATP regeneration. Response regulators (10 μM monomers) were added at time = 0, and time-point samples were resolved by Laemmli gel electrophoresis. Panels A–F show results for the indicated combinations.

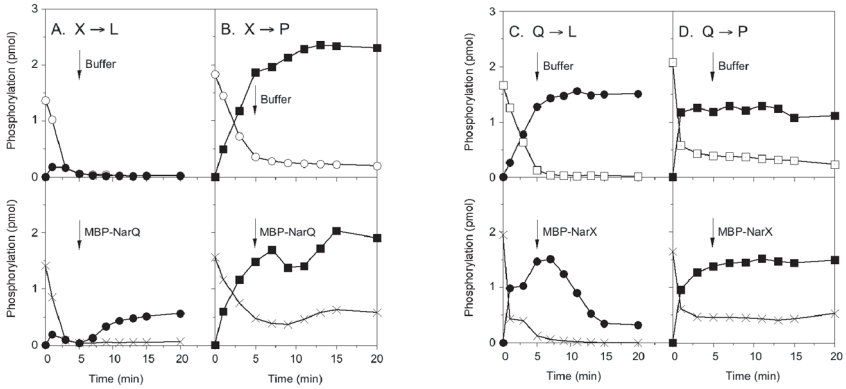

Fig. 4.

Multiple-round phosphoryl-transfer between Nar sensors and response regulators in the presence of nucleotides. Results are from a single representative experiment; others not shown generated similar patterns. ○, Phospho-MBP-$NarX_{227}$; □, phospho-MBP-$NarQ_{226}$; ×, phospho-MBP-Nar Sensor (when both were present); ●, phospho-His_6-NarL; ■, phospho-His_6-NarP. Sensors (0.5 μM dimers), prepared from gel filtration, were incubated with ^{32}P-ATP for autophosphorylation in the presence of ATP regeneration. Response regulators (10 μM monomers) were added at time = 0, and time-point samples were resolved by Laemmli gel electrophoresis. At the 5 min time point, the indicated component (buffer or MBP-Sensor dimers, 0.5 μM final concentration) was added.

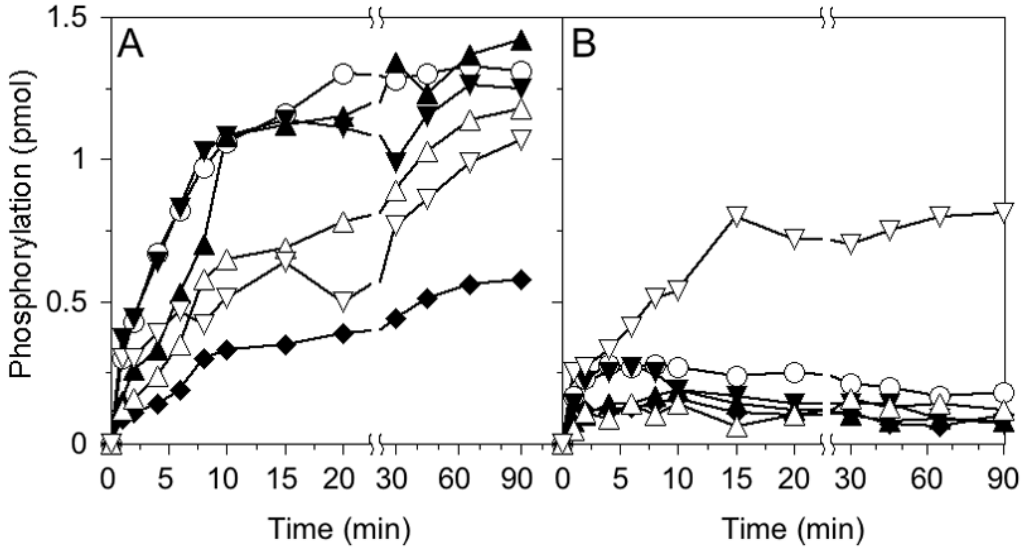

Fig. 5.

Autophosphorylation of wild-type and NarP-blind MBP-NarX proteins. Panels A and B show results from assays conducted in the presence and absence of ATP regeneration, respectively. Incorporated radiolabel was quantified by filter-binding as described in Experimental Procedures. Approximately 2.5 pmol of MBP-NarX dimers were present in each reaction. Results are from a single representative experiment; others not shown generated similar patterns. ○, Phospho-MBP-NarX; ▼, phospho-MBP-NarX(M411T); ▲, phospho-MBP-NarX(W442R); ◆, phospho-MBP-NarX(Q412R+M413V); △, phospho-MBP-NarX(K410E); and ▽, phospho-MBP-NarX(F452Y).

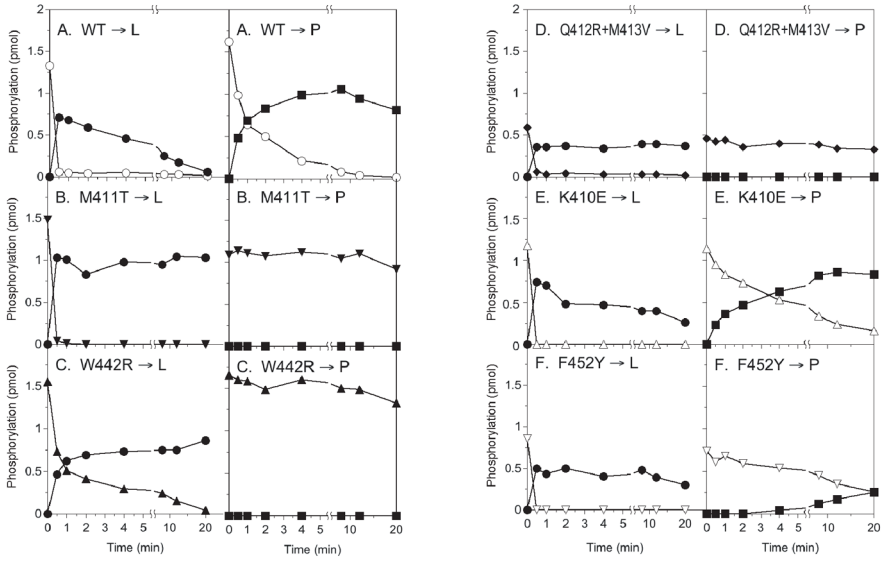

Fig. 6.

Phosphoryl-transfer between Nar sensors and response regulators at 4°C. Results are from a single representative experiment; others not shown generated similar patterns. ○, Phospho-MBP-NarX; ▼, phospho-MBP-NarX(M411T); ▲, phospho-MBP-NarX(W442R); ◆, phospho-MBP-NarX(Q412R+M413V); △, phospho-MBP-NarX(K410E); ▽, phospho-MBP-NarX(F452Y); ●, phospho-His_6-NarL; and ■, phospho-His_6-NarP. Sensors (0.5 μM dimers) were incubated at 19°C with ^{32}P-ATP for autophosphorylation in the presence of ATP regeneration. After equilibration to 4°Cm response regulators (10 μM monomers) were added at time = 0, and time-point samples were resolved by Laemmli gel electrophoresis. Panels A-F show results for the indicated combinations.

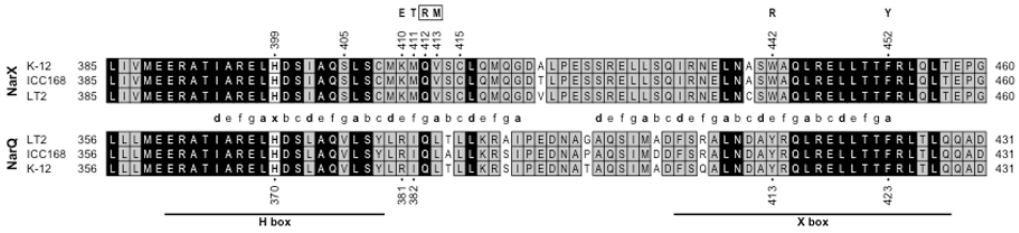

Fig. 7.

NarX and NarQ DHp domains. The NarP-blind substitutions are denoted with boldface letters above the *E. coli* NarX sequence. Numbers above and below the *E. coli* sequences show positions of mutational alterations described in this study, as well as the phosphoaccepting His residue (His-399 in NarX and His-370 in NarQ). Sequences are from *Escherichia coli* K-12 (GenBank accession number NC_000913), *Citrobacter rodentium* ICC168 (http://www.sanger.ac.uk), and *Salmonella enterica* LT-2 (NC_009137). The H box and X box motifs are defined in references (Wolanin *et al*., 2002) and (Hsing *et al*., 1998), respectively. Residues identical in all six sequences are indicated with black background, whereas residues identical in all three NarX or NarQ sequences are indicated with gray background. Lower-case letters between the NarX and NarQ sequences show the coiled-coil heptad positions from the DesK X-ray structure (Albanesi *et al*., 2009). The phosphoaccepting His residue occupies a skip position denoted here as “x” within the heptad repeats. Numbers to the left and right indicate positions of the terminal residues in the full-length sequences, which span 598 residues for NarX and 566 residues for NarQ.

Table 1

Effects of *narX* alterations on NarL- and NarP-dependent induction.

		β-Galactosidase sp act[a]					
		NarL-dependent induction by[d]			NarP-dependent induction by[e]		
Allele[b]	Region[c]	None	Nitrate	Nitrite	None	Nitrate	Nitrite
pHG165	—	35	40	30	140	170	170
narX^{+}	—	26	2060	120	1480	4340	4740
narQ^{+}	—	40	3360	3200	350	4920	4340
M411T	near H box	62	1840	1400	110	150[f]	120
W442R	X box	30	1820	1500	120	150[f]	110
Q412R+V413M	near H box	24	1800	810	110	270[f]	190
K410E	near H box	34	1350	1330	170	420[f]	270
F452Y	X box	45	2090	880	300	590[f]	380
M411V	near H box	21	2150	310	270	1010	750
S405P	H box	20	1700	720	220	1270	1830
C415R	near H box	79	1870	1090	640	1830	1350
S508C+D558V	N box, G box	1950	2010	3120	1000	1100	1380
V580A+F589I	G box	29	940	150	1460	1490	1460
K531I	D box	27	2640	460	1350	3330	2630
I343T	Central	100	2270	910	1540	3320	3780
R333L	Central	39	1340	1570	1540	3730	4420
L348P	Central	35	1760	750	1710	4850	4590
K481R+E586K	CA, G box	55	2350	820	1900	2890	3130
E586K	G box	30	2070	390	2120	3350	4010
K481R	CA	38	1810	440	2180	3290	3130
W442G	X box	120	1670	2380	2390	5230	5230
Y551F	G box	44	2250	830	3090	3360	4210
Q350R+T372A	Central	51	1890	570	3440	3310	3730
W442C	X box	180	1890	1530	4100	5260	4350

[a] Activity was measured as described in Experimental Procedures, and is expressed in Miller units.

[b] *narX* allele located on plasmid pVIS1241 derivative. The *narQ*$^{+}$ gene was on plasmid pVIS1231.

[c] Location of substitution(s) within NarX structure. Central, central module; DHp, dimerization and histidyl phosphotransfer domain; CA, catalytic and ATP-binding domain.

[d] Strain VJS5054 [Φ(*narG-lacZ*) Δ*narX narQ*::Tn*10*].

[e] Strain VJS5721 [Φ(*napF-lacZ*) Δ(*narXL*) *narQ*::Tn*10*].

[f] NarP-blnd phenotype as described in text.

Table 2

Effects of *narX* alterations on NarL-dependent repression.

	β-Galactosidase sp act[a]		
	NarL-dependent repression by[c]		
Allele[b]	**None**	**Nitrate**	**Nitrite**
pHG165	110	120	110
narX^{+}	120	40	120
M411T	93	43	50
W442R	97	30	56
S508C+D558V	45	22	26

[a] Activity was measured as described in Experimental Procedures, and is expressed in Miller units.

[b] *narX* allele located on plasmid pVJS1241 derivative.

[c] Strain VJS5768 [Φ(*frdA-lacZ*) Δ*narX narQ*::Tn*10*].

Table 3

Effects of NarX Q412R and V413M alterations on NarL- and NarP-dependent induction.

	β-Galactosidase sp act[a]					
	NarL-dependent induction by[c]			NarP-dependent induction by[d]		
Allele[b]	None	Nitrate	Nitrite	None	Nitrate	Nitrite
pHG165	11	10	17	220	230	120
narX^{+}	70	1800	120	1760	3340	3400
Q412R+V413M	100	1530	1300	450	500	400
Q412R	60	2090	220	450	1150	910
V413M	120	2330	1250	650	1740	2340

[a] Activity was measured as described in Experimental Procedures, and is expressed in Miller units.

[b] *narX* allele located on plasmid pVJS1241 or pVJS2474 derivative.

[c] Strain VJS5054 [Φ(*narG-lacZ*) Δ*narX narQ*::Tn*10*].

[d] Strain VJS5721 [Φ(*napF-lacZ*) Δ(*narXL*) *narQ*::Tn*10*].

Table 4

Effects of *narQ* alterations on NarL- and NarP-dependent induction.

	β-Galactosidase sp act[a]			
	NarL-dependent induction by[c]		NarP-dependent induction by[d]	
Allele[b]	None	Nitrate	None	Nitrate
pHG165	5	5	100	90
narQ$^+$	50	1220	220	3140
R381E	110	1120	260	2780
R381V	150	1340	360	3060
I382M	120	1230	500	2770
I382G	360	1050	3350	2450
I382S	390	1140	2860	2570
Y413R	5	7	70	210
F423Y	290	1030	3160	2400

[a] Activity was measured as described in Experimental Procedures, and is expressed in Miller units.

[b] *narQ* alleles located on plasmid pVJS1231 derivative.

[d] Strain VJS5054 [Φ(*narG-lacZ*) Δ*narX narQ*::Tn*10*].

[e] Strain VJS5721 [Φ(*napF-lacZ*) Δ(*narXL*) *narQ*::Tn*10*].

Mol Microbiol. Author manuscript; available in PMC 2011 February 6.

Table 5

Oligonucleotides.

Oligonucleotide	Sequence[a]	Purpose
ØHYL2726	5′–CATGAAGATGCGGGTGAGTTGTT	NarX(V413) revertant (coding strand)
ØHYL2727	5′–AACAACTCACCCGCATCTTCATG	NarX(V413) revertant (template strand)
ØHYL2728	5′–TGAAGATGCAGATGAGTTGTTTA	NarX(Q412) revertant (coding strand)
ØHYL2729	5′–TAAACAACTCATCTGCATCTTCA	NarX(Q412) revertant (template strand)
ØJSnarL-1	5′–GCAAAGGATCCAATCAGGAACCGGCTACTATC	His_6-NarL (coding strand)
ØJSnarL-2	5′–CGCATCATCGAAGCTTTGGGAACCGTAATCAGA	His_6-NarL (template strand)
ØJSnarP-1	5′–CAGCGGATCCCTGAAGCAACACCTTT	His_6-NarP (coding strand)
ØJSnarP-2	5′–ATCGTCGGCAAGCTTCGGGCTATTTTTATT	His_6-NarP (template strand)
ØLLC2560	5′–GCTCTAGATACCGTTCGCTGGAAGCGTCAGTAG	MBP-$NarQ_{226}$ (coding strand)
ØLLC2562	5′–CCCAAGCTTCTACATTAACTGACTTTCCTCACCCTC	MBP-$NarQ_{226}$ (template strand)
ØLLC2565	5′–GCTCTAGATATGCCGTACTTGAGCAGCGGGTTCAGG	MBP-$NarX_{227}$ (coding strand)
ØLLC2567	5′–CCCAAGCTTCTACTCATGGGTATCTCC	MBP-$NarX_{227}$ (template strand)
ØLLC2980	5′–CAGGTACTTTCTTACTTAGAGATCCAGTTGACGTTACTGAAGCG	NarQ(R381E) substitution (coding strand)
ØLLC2981	5′–GTAACGTCAACTGGATCTCTAAGTAAGAAAGTACCTGAGC	NarQ(R381E) substitution (template strand)
ØLLC2982	5′–GTTGAATGATGCTCGCCGGCAGTTACGC	NarQ(Y413R) substitution (coding strand)
ØLLC2983	5′–GCGTAACTGCCGGCGAGCATCATTCAAC	NarQ(Y413R) substitution (template strand)
ØLLC2984	5′–GCTGTTGACTACTTACCGCCTGACGCTG	NarQ(F423Y) substitution (coding strand)
ØLLC2985	5′–CAGCGTCAGGCGGTAAGTAGTCAACAGC	NarQ(F423Y) substitution (template strand)
ØLLC2992	5′–CTGGCTCAGGTACTTTCTTACTTANNNATCCAGTTGACGTTACTGAAG	NarQ(R381) randomization (coding strand)
ØLLC2993	5′–GAAAGTACCTGAGCCAGCGAGTC	NarQ(R381 & I382) randomization (template strand)
ØLLC2994	5′–CAGGTACTTTCTTACTTACGTNNNCAGTTGACGTTACTGAAGCGTTC	NarQ(I382) randomization (coding strand)

[a]Underlined sequence denotes introduced restriction endonuclease sites or codon substutions.